Extreme Mechanics Letters 40 (2020) 100928

Contents lists available at ScienceDirect

Extreme Mechanics Letters

journal homepage: www.elsevier.com/locate/eml

Computational insights into the influence of substrate stiffness on collective cell migration

Daniel Garcia-Gonzalez [a,*], Arrate Muñoz-Barrutia [b,c]

[a] Department of Continuum Mechanics and Structural Analysis, Universidad Carlos III de Madrid, Avda. de la Universidad 30, 28911 Leganés, Madrid, Spain
[b] Department of Bioengineering and Aerospace Engineering, Universidad Carlos III de Madrid, Avda. de la Universidad 30, 28911 Leganés, Madrid, Spain
[c] Instituto de Investigación Sanitaria Gregorio Marañón, Calle de O'Donnell, 48, 28009 Madrid, Spain

ARTICLE INFO

Article history:
Received 4 June 2020
Received in revised form 28 July 2020
Accepted 8 August 2020
Available online 15 August 2020

Keywords:
Collective cell migration
Continuum model
Stiffness gradient
Finite element method
Cell polarisation

ABSTRACT

Critically important biological phenomena in health and disease, such as wound healing, cancer metastasis, and embryonic development, are governed by collective cell migration. This highly complex process depends not only on cellular features, but also on different stimuli from the local cell environment. Cell migration is promoted by the combination of physico-chemical cues, including the mechanical properties of the extracellular matrix (ECM). Stiffness gradients within ECM have recently been demonstrated to result into preferred directions of cell migration. However, the specific mechanisms driving this directed collective cell migration and their relative roles remain unclear. Here, we develop a continuum formulation and its finite element (FE) implementation to test different hypotheses on the cause of spatial heterogeneities during cell migration on heterogeneous-stiffness substrates. We evaluate two key hypotheses: (i) cell polarisation is promoted by stiffness gradients within the ECM and; (ii) propulsion forces are weighted by ECM stiffness. Ultimately, we provide a robust *in silico* framework to explain experimental observations and guide future research.

1. Introduction

During a number of biological processes such as embryonic development and wound healing, cells carry out their functions at two levels: as individual entities and as a collective. *In vivo*, cells do not exist in isolation but in constant contact with other cells and the extracellular matrix (ECM) or basement membrane, through which they can migrate [1]. Thus, while the understanding of the dynamics of individual cells is essential, the comprehension of the dynamics of cell aggregates is often the most physio-pathological relevant mode of migration [2]. These multicellular processes present high complexity involving different physico-chemical cues, among which mechanics plays a major role. The mechanical processes regulating collective migration include crosstalk between cell-cell and cell-ECM adhesive interactions, and corresponding active responses from cell contractility [1]. In a recent article, Alert and Trepat [3] examined the different mechanical features occurring during collective cell migration. These authors classified the acting forces in two main groups: positional and orientational. Among the former, cellular interaction forces include adhesion, friction, repulsion and active forces due to polarity and actomyosin-based contractility [4–6]. Another important contribution to positional forces stems from interactions between cells and their substrate. These forces mainly arise from active traction forces due to cell adhesion to the substrate and friction [7]. Moreover, interactions between cells promote changes in their shape and polarisation alignment. This cell polarisation induces a preferred orientation within the cell aggregates, which is also significantly affected by the mechanical properties of the substrate (i.e., stiffness magnitude and spatial distribution) [8–10].

One of the most challenging problems to understand the role of mechanics on collective cell migration is the influence of heterogeneous stiffness and stress distributions within the cell substrate. In this regard, an anisotropic and/or heterogeneous ECM microstructure results into non-homogeneous external mechanical forces acting on the cell continuum [11]. From a mechanical balance analysis, it is clear that such mechanical constraints interplay with the internal stresses within the cell continuum leading to cellular reorientations and guiding the collective migration. Furthermore, local cellular stresses and/or reorientations can be transmitted over long distances within the continuum making use of mechanical cell–cell communication [12,13]. A consequence of mechanical balance under heterogeneous ECM conditions, which has been experimentally demonstrated, is that

* Corresponding author.
E-mail address: danigarc@ing.uc3m.es (D. Garcia-Gonzalez).

https://doi.org/10.1016/j.eml.2020.100928

cells trend to migrate along gradients of substrate stiffness [14]. This preferential cell movement to stiffer regions – termed durotaxis – is postulated to contribute to cell migration in wound healing [15]. This process is mediated by actomyosin cellular traction forces and focal adhesions promoting cell attachment to ECM [9]. Breckenridge et al. [9] suggested that traction forces could be explained by a cell polarisation process guided by stiffness gradients, and postulated that this polarisation is a potential mechanism underlying durotaxis. In related work, Bun et al. [8] demonstrated that shape polarisation can be triggered and directed by stiffness sensing through single localised integrin-mediated cues. More recently, Sunyer et al. [16] conducted experiments to test the influence of substrate stiffness gradients on collective cell migration. These results show that stiffness gradients within the substrate promote non-symmetric migration towards the stiffer regions.

Motivated by these works, we propose a novel constitutive model formulated within a consistent finite element (FE) framework for finite deformation to simulate collective cell migration on heterogeneous-stiffness substrates. This model incorporates original dependences of external mechanical forces and cell polarisation on substrate stiffness. The FE model is implemented within a fully implicit framework and used to simulate collective cell migration of epithelial monolayers. The model parameters are first identified from experimental measurements published in the literature. Then, we simulate the experiments reported by Sunyer et al. [16] for collective migration on homogeneous substrates. After validation of the model predictions against such experiments, two different hypothetical driving forces guiding non-symmetric collective migration are tested: (i) cell polarisation is promoted by stiffness gradients within the cell substrate; (ii) propulsion forces are weighted by cell substrate stiffness. The computational results reported here suggest that polarisation induced by substrate stiffness gradients is sufficient to promote non-symmetric collective migration. Overall, the proposed model provides good predictions of collective migration along time and stress distribution within the cell under different substrate conditions, representing a powerful tool to guide future experimental research.

2. Continuum model formulation

Current computational approaches describe the cell migration process from different perspectives: at the cellular scale [17,18] and at the continuum scale [19–22]. The latter considers cell-aggregates as a continuum body where intracellular as well as intercellular interactions are treated as internal stresses. Thus, local mechanical stimuli at the cellular level can be globally transmitted in the form of mechanical waves transporting interaction forces within the cell "continuum". In parallel to these mechanical waves, some existing models couple other physics such as actomyosin concentration and cell polarisation evolution through non-local approaches [21]. Although significant efforts have been made to date to model the mechanics of collective cell migration, only few models account for the effects of stiffness gradients within the ECM or the substrate. A relevant work accounting for them was published by Escribano et al. [23]. This model is formulated for 1D and is based on the combination of truss elements and a particle-based approach to simulate the dynamics of cell–matrix adhesions and cell–cell interactions. The same research group published another important work [22] where a continuum material model is coupled to an agent-based approach. These works, despite of their indisputable relevance, are computationally expensive and need of discrete models running in parallel to the continuum approach.

A significant work by Ladoux and Mège [1] highlights two main mechanisms as promoters of collective dynamics: collective cell polarisation and coordinated contractile processes. Here, we incorporate in a novel fashion the influence of substrate stiffness gradients on cell polarisation and postulate this process as the main promoter of non-symmetric collective migration. We propose a 3D purely continuum formulation (suitable to be simplified to 1D) to address collective cell migration on heterogeneous-stiffness substrates in physiological environments. To this end, we take a recent model proposed by Banerjee and Marchetti [21] as the starting point. Note that the present work is devoted to the comprehension of the specific mechanisms leading to spatial non-symmetries during cell migration due to heterogeneous mechanical properties within the substrate. Hence, the proposed modelling framework extends previous models to include such dependencies while, without the loss of generality, simplifies other specific features to isolate and focus the analysis. Moreover, cell proliferation is neglected as cell division has been reported to be independent of substrate stiffness and it is inhibited in the experimental work taken here as reference [16]. We then formulate the problem on two cornerstones: mechanical balance; and non-local evolution of cell polarisation. The mechanical balance assumes negligible inertial effects and, in its spatial form, reads as:

$$h\nabla \cdot \boldsymbol{\sigma} + \boldsymbol{T} = \boldsymbol{0} \tag{1}$$

where ∇ is the spatial gradient and $h = \lambda_{op} h_o$ is the deformed height of the cell monolayer, with λ_{op} and h_o being the out-of-plane stretch and the initial height, respectively. The mechanical stress within the monolayer is described, in its deformed state, by the Cauchy stress tensor $\boldsymbol{\sigma}$. The term $\boldsymbol{T}$ describes the external body forces per unit length.

The stress within the cell-aggregates is defined by a constitutive equation. In this work, we make use of hyperelasticity to derive the stress tensor from a free energy potential formulated for finite deformation (essential to account for large deformations and mechanical non-linearities). This free energy can be understood as the combination of different contributions arising from specific mechanisms. Ideally, a complete description of the problem should include: (1) a pure elastic component accounting from isochoric and volumetric resistance to deformation due to cell–cell adhesions; (2) a viscoelastic component accounting for cell junctions remodelling; (3) a purely viscous component accounting for cell–cell friction and repulsion forces; and (4) an active anisotropic component related to the concentration of contractile actomyosin. Here, we adopt a simplified energy potential to reduce the internal cell stresses to an averaged component due to cell–cell adhesions. This reduces the number of model parameters to the minimum and facilitates the analysis of substrate stiffness influence limiting other effects (i.e., relaxation dependences, anisotropic responses). To this end, a neo-Hookean potential in the following form is chosen:

$$\Psi\,(\boldsymbol{F}) = \frac{\mu_{cell}}{2}\,[I_1 - 3] \tag{2}$$

where $\boldsymbol{F}$ is the deformation gradient, $I_1 = trace(\boldsymbol{F}^{\boldsymbol{T}}\boldsymbol{F})$ is the first invariant of the right Cauchy–Green deformation tensor and μ_{cell} is the apparent shear modulus of the cell aggregate describing the "stiffness" of the cell continuum to deform. Therefore, the continuum mechanical behaviour is implicitly related to both the cell stiffness and cell–cell adhesion. From thermodynamics principles and assuming incompressibility, the Cauchy stress tensor can be derived as:

$$\boldsymbol{\sigma} = -\Pi\boldsymbol{I} + \frac{\partial \Psi}{\partial \boldsymbol{F}}\boldsymbol{F}^{\boldsymbol{T}} = -\Pi\boldsymbol{I} + \mu_{cell}\boldsymbol{F}\boldsymbol{F}^{\boldsymbol{T}} \tag{3}$$

where $\boldsymbol{I}$ is the second order unit tensor and Π is a Lagrange multiplier (related to volumetric pressure). Note that the proposed

framework allows for the definition of other complex constitutive equations by simply changing the conceptualisation of the energy potential Ψ. Thus, an additive composition of Ψ can be used to add viscoelastic (see Ref. [24] for consistent continuum visco-hyperelastic formulation) or active components (see Ref. [21]). Regarding the external mechanical forces affecting the cell-aggregates ($\boldsymbol{T}$), they are mainly due to cell-substrate interactions. Therefore, it seems convenient to split this contribution into a first component due to cell-substrate friction, and a second component related to propulsion forces generated by the cell-substrate adhesion:

$$\boldsymbol{T} = -\zeta \dot{\boldsymbol{u}} + f\boldsymbol{p} \tag{4}$$

where ζ is a friction coefficient, $\dot{\boldsymbol{u}}$ is the velocity field defined as the time derivative of the displacement field $\boldsymbol{u}$, $\boldsymbol{p}$ is the polarisation, and f is the propulsion force per unit cross-sectional area. According to Alert et al. [20], this coefficient is related to the maximal traction stress exerted by polarised cells on the substrate. Maximum care must be taken here when formulating the collective migration as a finite deformation problem. One important aspect is that the effective f is expressed as a force per unit current cross-sectional area (accounting for variations of such an area during continuum deformation). Another important consideration for this work is that such traction stress f can, a priori, be considered dependent on the substrate stiffness as implicitly assumed by Sunyer et al. [16]. This hypothesis is also motivated by experimental work which suggests that durotaxis may be triggered by higher traction forces on stiffer substrates [9,25–27]. Therefore, the external mechanical sources are rewritten here as:

$$\boldsymbol{T} = -\zeta \dot{\boldsymbol{u}} + \tilde{f}(E_s)\boldsymbol{p} \tag{5}$$

where $\tilde{f}(\boldsymbol{x}) = f_{ref} + \xi \frac{E_s(\boldsymbol{x})}{E_{s,ref}}$ is the traction stress dependent on the linearised stiffness (Young's modulus) of the substrate E_s, with $E_{s,ref}$ being a reference Young's modulus of the substrate, ξ a constant parameter and $\boldsymbol{x}$ the spatial coordinates. This later dependence is assumed, as a first approach, in a similar trend than in the model proposed by Alert and Casademunt [28]. However, future variations may be included to capture further effects such as a decrease of durotaxis with an increase of average stiffness (while keeping the same stiffness gradient magnitude) [16,22]. This work focuses on the effects of stiffness gradients within the substrate. This is why the variable $E_s(\boldsymbol{x})$ depends on the spatial coordinates. The description of the substrate stiffness depending on the spatial coordinates is based on the following assumptions: (i) the spatial distribution of the substrate stiffness can be defined by the appropriate function, in a reference undeformed configuration that depends on the substrate material coordinates $\boldsymbol{X_s}$; (ii) during collective cell migration, although large deformations of the cell continuum are expected, small deformations are assumed for the substrate leading to the relation of substrate's coordinates $\boldsymbol{x_s} = \boldsymbol{X_s} + \boldsymbol{u_s} \approx \boldsymbol{X_s}$, where $\boldsymbol{u_s}$ is the displacement field within the substrate; (iii) therefore, the spatial coordinates of the cell-aggregates correspond to the material coordinates of the substrate as $\boldsymbol{x} = \boldsymbol{X} + \boldsymbol{u} \approx \boldsymbol{X_s}$. Overall, we assume large deformations within the cellular substrate but small deformations within the substrate. Therefore, as the cellular continuum migrates over the substrate overcoming frictional forces, the cellular spatial coordinate $\boldsymbol{x}$ will correspond to the substrate material coordinate $\boldsymbol{X_s}$. It is worth to mention that for other cases involving very soft substrate this assumption may be not true, but this problem would require a different approach simulating in a lower scale the cellular-substrate interactions.

Note that the mechanical balance depends on the polarisation $\boldsymbol{p}$. Therefore, the complete description of the problem requires a consistent flow rule for this variable. To this end, a non-local evolution of $\boldsymbol{p}$ is defined as:

$$\dot{\boldsymbol{p}} = \kappa \nabla^2 \boldsymbol{p} + \gamma \nabla E_s(\boldsymbol{x}) \tag{6}$$

where κ is a diffusion-like coefficient describing the influence of neighbouring cells on local polarisation and γ is a coefficient describing the sensitivity of the cell-aggregates to polarise along the stiffness gradient of the substrate. The first term is motivated by the fact that cell–cell contact triggers cell polarisation, and these interaction forces are transmitted within the cell continuum leading to a diffusion-like process resulting into a non-local evolution of cell polarisation [9]. The second term is motivated by experimental observations which show that stiffness sensing cues are sufficient to trigger and direct shape polarisation [8,9,16]. Other terms could be added to incorporate polarisation dependencies on ATP driven processes, velocity dependent advective terms, actomyosin concentration or relaxation processes (see Ref. [21]).

The proposed model allows for its implementation in a fully coupled FE framework. To this end, a fully implicit integration algorithm is formulated and implemented (see Appendix for details). Overall, the present work provides a robust FE framework to computationally test potential effects of substrate stiffness gradients on collective cell migration. In addition, as previously indicated, the present formulation allows to incorporate other relevant physical mechanisms into the global formulation.

Table 1
Common constitutive parameters used in all simulations. These parameters are directly identified from experimental measurements reported in the literature [16,20,29–32].

Constitutive parameters				
μ_{cell} (kPa)	ζ (nNμm^{-3}s)	ξ_{ref} (kPa)	h_o (μm)	κ (μm^2)
2.5	1	0.25	6	0.3

3. Results

This section evaluates the predictive capability of the model presented. The model parameters are first identified from experimental measurements. This set of parameters is used to validate the model against experimental data of collective cell migration on homogeneous-stiffness substrates. Then, the model hypotheses are tested and computational predictions for collective cell migration on heterogeneous-stiffness substrates are compared to relevant experimental data. Finally, the proposed driving forces for non-symmetric collective cell migration are further analysed.

3.1. Model predictions for homogeneous-stiffness substrates

First, the model parameters for the specific cell continuum modelled, the epithelial monolayer, are identified from the literature to avoid ad-hoc calibration by fitting. The initial monolayer height is commonly reported with a value between 5–7 μm [16,29]. The epithelial tissue exhibits a shear modulus ranging from 2 to 8 kPa [30]. A common maximal value of 0.2–0.5 kPa for the traction stresses ($\tilde{f}$) has been reported in the literature [29,31]. Moreover, the friction coefficient has been experimentally estimated with a value of 1 nNμm^{-3}s [32]. Therefore, the model parameters used in this work are directly defined from reported experimental measurements, see Table 1. Note that the diffusion-like coefficient related to polarisation is chosen to consistently describe its experimental distribution within epithelial monolayers.

To perform simulations, we need to define the FE domain and the corresponding boundary conditions. In Fig. 1, a schematic

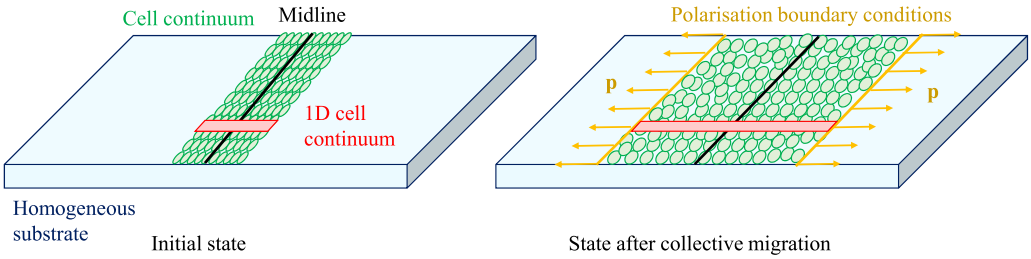

Fig. 1. Schematic representation of the continuum model for: cell continuum (green) on homogeneous substrate at the initial state and after collective migration. The polarisation boundary conditions are indicated in the right part of the figure. The 1D cell continuum (red) illustrates the representative one dimensional domain taken for the FE simulations. (For interpretation of the references to colour in this figure legend, the reader is referred to the web version of this article.)

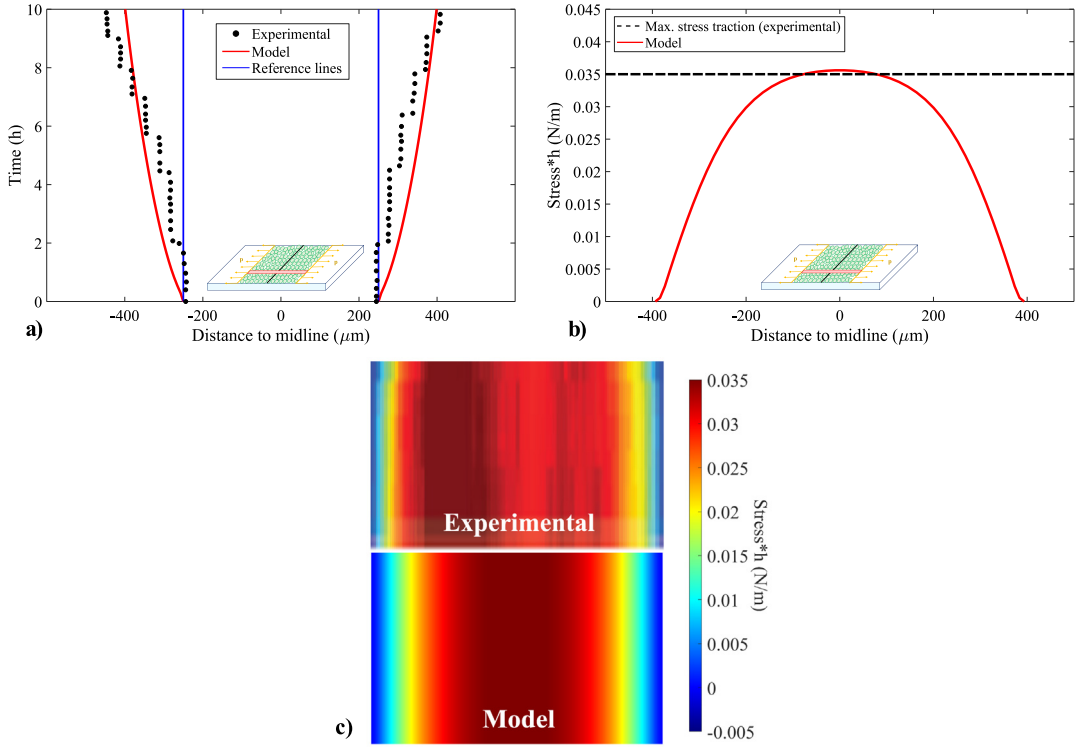

Fig. 2. Comparison between experimental data [16] and model predictions of collective cell migration on homogeneous substrate: (a) collective cell expansion along time; (b) stress traction predictions and maximum stress traction observed experimentally; (c) comparison between experimental data [16] and model predictions of the stress tractions spatial distribution. Note that these results are independent of the model parameters γ, ξ and $E_{s,ref}$.

representation of the initial and final stages of collective cell migration on a homogeneous-stiffness monolayer is presented. Here, the cell continuum is represented as an in-plane monolayer with an initial constant heigh that propagates on the substrate. Therefore, if no instabilities are considered, this domain can be reduced to a representative 1D domain (see 1D cell continuum in red, Fig. 1). According to this scheme, free mechanical boundary conditions by means of displacement fields are imposed. The mechanical boundary conditions are completed by defining free stress surfaces on the leading edges, as experimentally reported [16]. Furthermore, following experimental observations and previous computational approaches [20], constant polarisation boundary conditions are imposed on the leading edges equal to unit normal vector. In addition, both time and spatial convergences have been verified in all the simulations presented.

Once the complete FE model is defined, we first simulate cell collective migration on a homogeneous-stiffness substrate reproducing the experiments reported by Sunyer et al. [16]. The comparison between model predictions and experimental results is shown in Fig. 2. These results are independent of the model parameters γ, ξ and $E_{s,ref}$, as the substrate stiffness along the whole domain is constant. In addition, all the model parameters used at this stage are consistent and directly identified from experimental observations reported in the literature. In Fig. 2a, a symmetric collective migration is observed leading to a continuous continuum expansion. The model predictions reproduce with a very good agreement not only the experimental quantitative migration, but also its evolution along time. Moreover, a very good agreement is observed by means of stress distribution within the cell continuum (Fig. 2b,c). The model predicts the same maximum stresses within the cell-aggregates and also the reduction to null stress at the leading edges [16]. Overall, with direct identification of the constitutive parameters from experimental measurements, the model provides good predictions of the collective cell migration on homogeneous-stiffness substrates by means of both migration evolution with time and stress distribution within the cell continuum.

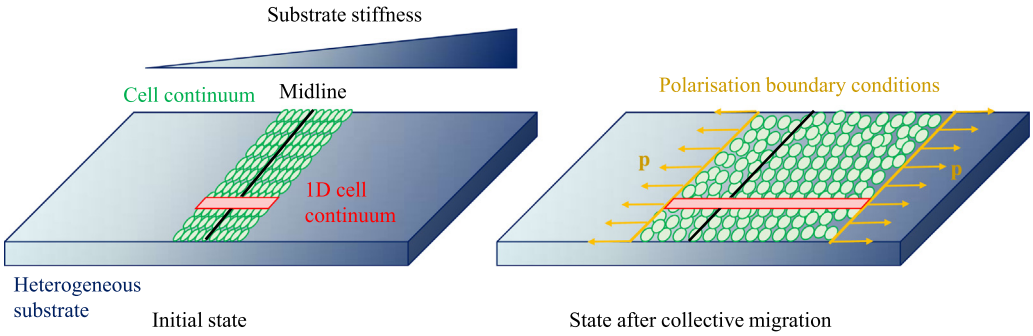

Fig. 3. Schematic representation of the continuum model for: cell continuum (green) on linearly-variant stiffness substrate at the initial state and after collective migration. The polarisation boundary conditions are indicated in the right part of the figure. The 1D cell continuum (red) illustrates the representative one dimensional domain taken for the FE simulations. (For interpretation of the references to colour in this figure legend, the reader is referred to the web version of this article.)

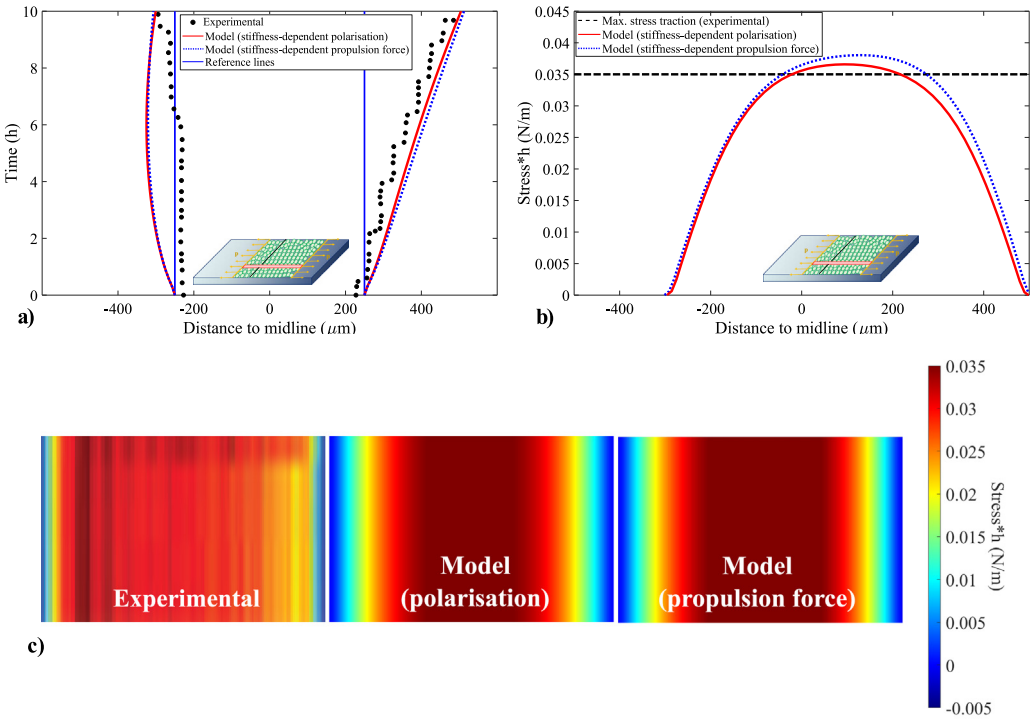

Fig. 4. Comparison between experimental data [16] and model predictions of collective cell migration on stiffness-heterogeneous substrate: (a) collective cell expansion along time; (b) stress traction predictions as a function of time and maximum stress traction observed experimentally; (c) comparison between experimental data [16] and model predictions of the stress tractions spatial distribution. The parameters used are the ones in Table 1. In addition, for stiffness-dependent polarisation predictions: $\gamma = 0.01$ μm/MPa; $\xi = 0$ Pa; and for stiffness-dependent propulsion force predictions: $\gamma = 0$ μm/MPa; $\xi = 8$ Pa; $E_{s,ref} = 8$ kPa.

3.2. Model predictions for heterogeneous-stiffness substrates

Once the model has been tested under homogeneous-stiffness substrate conditions, we evaluate next its capability to predict non-symmetric migration under stiffness-heterogeneous substrate conditions. To this end, we make use of relevant experiments conducted by the same authors but employing heterogeneous substrates [16]. In such experiments, collective migration in epithelial monolayers is studied on substrates with a constant stiffness gradient of 57.5 MPa/m. A schematic representation of these results is presented in Fig. 3. According to this scheme, a similar reduction of the problem formulation to 1D can be done as explained in the previous section. The mechanical and polarisation boundary conditions applied in these simulations are the same as those for homogeneous-stiffness substrates. However, the substrate stiffness $E_s(\boldsymbol{x})$ is not constant anymore but depends on the current spatial coordinate $\boldsymbol{x}$ of the cell continuum element. Therefore, the last term of Eq. (6) is now relevant for the polarisation evolution during the migration process. In addition, the propulsion force in Eq. (5), $\tilde{f}(E_s)$, is also non-constant and depends on the current location of each cell continuum element.

The analysis conducted here aims at isolating two potential driving forces of non-symmetric collective migration: (i) polarisation induced by stiffness gradients within the substrate; (ii) propulsion force dependent on local substrate stiffness. Therefore, a first set of simulations is conducted for the hypothesis (i) where we adopt non null values for the parameter γ and $\xi = 0$ Pa (i.e., constant propulsion force within the substrate). These simulations provide a discussion on "whether stiffness-gradient-induced polarisation" can result into non-symmetric migration. Moreover, a second set of simulations is conducted for the hypothesis (ii) where we adopt non null values for the parameter ξ

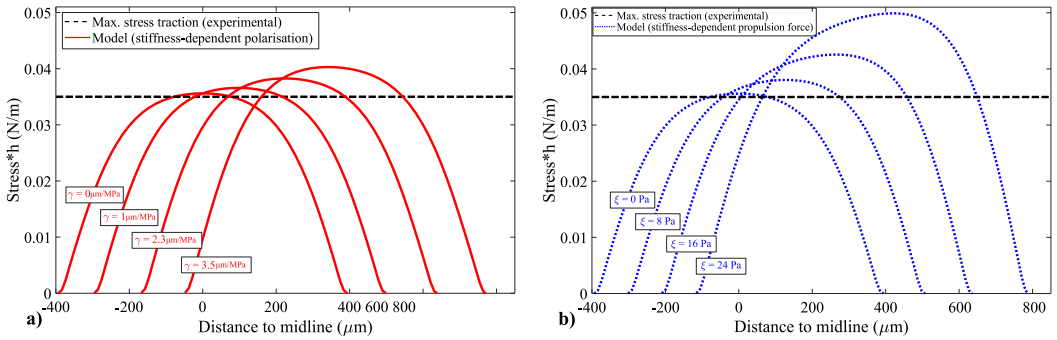

Fig. 5. Parametric analysis in terms of stress traction distributions as a function of the distance to reference midline for: (a) the stiffness-sensitivity polarisation parameter γ; (b) the stiffness-sensitivity propulsion force parameter ξ. Note that the range used for the parametric analyses lead to similar displacements of the cell-continuum leading edge. The parameters used are the ones in Table 1. In addition, for stiffness-dependent polarisation predictions, (a): $\xi = 0$ Pa and the γ shown; and for stiffness-dependent propulsion force predictions, (b): $\gamma = 0$ μm/MPa and the ξ shown in the figure.

and $\gamma = 0$ μm/MPa (i.e., polarisation independent of stiffness gradients). These simulations provide a discussion on whether "propulsion force dependence on stiffness" can result into non-symmetric migration. The computational results for both cases are compared to experimental observations [16] in Fig. 4. After calibration of these parameters, the model can accurately describe the experimentally observed collective cell migration for both hypotheses (Fig. 4a). Although both approaches may describe similar trends by means of collective migration, they provide differences for the stress distribution (Fig. 4b,c). Experimental results for stiffness gradient substrates show almost identical maximum values compared to homogeneous substrates [16]. In this regard, the first hypothesis (i), stiffness-gradient-dependent polarisation, predicts a slight increase in stress with respect to the results provided for homogeneous substrates. However, the second hypothesis (ii), stiffness-dependent propulsion force, predicts a more relevant increase in maximum stress within the cell continuum. These results suggest a better fit of the hypothesis (i), which is in good agreement with experiments published by Joaquin et al. [33], and are further analysed in next section.

3.3. Analysis of the potential driving forces guiding non-symmetric collective migration

This section provides a parametric analysis of the two relevant model parameters governing the two driving forces for non-symmetric collective cell migration: (i) γ for stiffness gradient-dependent polarisation; (ii) ξ for stiffness-dependent propulsion force. From the previous section it was inferred that both approaches can provide the same results by means of effective migration along time. However, these approaches result into different stress distributions within the cell continuum. Therefore, this study focuses on the effect of the aforementioned parameters on cell stresses. To provide a relevant comparison, the parameters are varied within a range so that both approaches predict the same migration levels.

Fig. 5 presents the stress distribution along the space coordinates occupied by the cell continuum at the end of the simulation for different conditions. A parametric analysis isolating the effects of polarisation sensitivity to stiffness gradient of the substrate is shown in Fig. 5a, where the parameter γ is changed while fixing $\xi = 0$ Pa. Higher values of γ represent a faster cell polarisation along stiffness gradient direction resulting into larger displacement of the continuum to such stiffer region. Accompanying this stronger migration, a slight increase in stress is observed with a symmetric distribution within the deformed configuration of the cell-aggregates. Moreover, Fig. 5b shows the parametric analysis isolating the effects of propulsion force sensitivity to substrate stiffness by changing the parameter ξ and fixing $\gamma = 0$ μm/MPa. Higher values of ξ represent a stronger dependence of the propulsion force on substrate stiffness and, similar to the effect of γ, result into larger displacement of the continuum to such stiffer region. However, the stress distribution within the cell continuum develops differently leading to a significant increase in magnitude and to a non-symmetric distribution within the deformed continuum, presenting higher values close to the leading edge in the stiffer region. Overall, these results show that different mechanisms can equally explain the collective migration processes but they will have completely different consequences in the mechanical balance. The stress distribution within the cell continuum is very relevant as may open stretch activated channels or promote biological processes such as the rate and orientation of cell division [34]. This computational model could serve as an *in silico* tool helping at elucidating potential mechanisms involved in collective cell migration and guiding future experimental research.

4. Conclusions

Collective cell migration is an essential process during important biological events such as wound healing and embryonic development. This process has been demonstrated to significantly depend on mechanical cues. Although significant efforts have been made to date proposing computational models to simulate such events, only few works account for stiffness gradients within the cell substrate [16,22,23]. Here, we postulate that the influence of substrate stiffness gradients on cell polarisation is the main promoter of non-symmetric collective migration and incorporate it in a continuum formulation. To this end, we propose a consistent constitutive model for finite deformations, incorporating original dependences on substrate stiffness, and provide the corresponding finite element (FE) formulation. This FE model is implemented within a fully implicit framework and used to simulate collective cell migration of epithelial monolayers. First, the model parameters are directly identified from relevant experimental observations. This set of parameters is used to simulate the experiments reported by Sunyer et al. [16] for collective migration on homogeneous substrates. The model predictions provide a very good agreement with experiments, including spatial migration as a function of time and stress distribution within the cell continuum. Then, the validated model is used to test two different hypothetical driving forces guiding non-symmetric collective migration: (i) cell polarisation is promoted by stiffness gradients within the cell substrate; (ii) propulsion forces are weighted by cell substrate stiffness. These results along with a

parametric study for these incorporated dependences on substrate stiffness show that, although different mechanisms may explain the collective migration, they also lead to different consequences in the mechanical balance. In this regard, the first hypothesis (i) predicts a symmetric stress distribution within the cell continuum with a slight increase in magnitude for higher substrate stiffness gradients. Moreover, the second hypothesis (ii) predicts non-symmetric stress distributions and a strong increase in magnitude for higher stiffness gradients. According to experimental observations published by Sunyer et al. [16] that show almost identical cell stresses for homogeneous and heterogeneous substrates, we suggest polarisation induced by substrate stiffness gradients as a firm candidate to drive collective cell migration.

Finally, it is worth to mention that the proposed model has consciously been simplified to isolate the analysed effects of substrate stiffness. In this regard, the model formulation, in its current form, may present limitations to predict other collective migration scenarios. However, note that this formulation allows for the incorporation of active forces arising from actomyosin concentration, proliferation, rate dependences along with relaxation processes within the cell continuum mechanical response or further dependences of the polarisation flow rule. As closing statement, we want to highlight the potential use of this computational model as an *in silico* tool to help and guide future experimental research.

Declaration of competing interest

The authors declare that they have no known competing financial interests or personal relationships that could have appeared to influence the work reported in this paper.

Acknowledgements

The authors thank Denis Wirtz (Johns Hopkins University) for relevant discussion. The authors acknowledge support from Programa de Apoyo a la Realizacion de Proyectos Interdiscisplinares de I+D para Jovenes Investigadores de la Universidad Carlos III de Madrid and Comunidad de Madrid, Spain (project: BIOMASKIN). DGG acknowledges support from the Talent Attraction grant, Spain (CM 2018 - 2018-T2/IND-9992) from the Comunidad de Madrid. This work was partially funded by projects TEC2015-73064-EXP and TEC2016-78052-R from the Spanish Ministry of Economy and a 2017 Leonardo Grant for Researchers and Cultural Creators, BBVA Foundation, Spain.

Appendix. Generalised finite element framework

Hereafter, the formulation is presented in index notation to facilitate the implementation. Indexes with capital letters, i.e., $\{I, J, K, L\}$, represent material coordinates; while indexes with lower case letters, i.e., $\{i, j, k, l\}$, represent spatial coordinates. The independent variables of the problem are the mechanical displacement field $\boldsymbol{u}$, the polarisation vector $\boldsymbol{p}$, and the Lagrange multiplier Π. Other extensions of the model would incorporate actomyosin concentration and viscoelastic internal variables as independent variables as well.

A.1. Strong forms

The strong forms of the mechanical balance and the polarisation flow rule residuals, Eqs. (1) and (6), can be expressed in the deformed configuration Ω as:

$$\begin{aligned} Res_i^u &= h\sigma_{ij,j} - \zeta \dot{u}_i + \tilde{f} p_i = 0 \quad in\ \Omega \\ Res_i^p &= \dot{p}_i - \kappa \left(p_{i,j}\right)_{,j} - \gamma E_{s,i} = 0 \quad in\ \Omega \\ Res^{\Pi} &= \Pi\,(J-1) = 0 \quad in\ \Omega \end{aligned} \tag{A.1}$$

where $J = det(\boldsymbol{F})$ is the Jacobian. Moreover, the deformation gradient can be written by means of the displacement field as:

$$F_{ij} = u_{i,J} + I_{ij} \tag{A.2}$$

A.2. Spatial and temporal discretisation, and weak forms

We estimate the spatial discretisation of the finite element test functions ($\boldsymbol{\delta p^e}$, $\boldsymbol{\delta p^e}$ and $\delta\Pi^e$) and trial functions ($\boldsymbol{u^e}$, $\boldsymbol{p^e}$ and Π^e) from the nodal values as:

$$\begin{aligned} \boldsymbol{\delta p^e} &= \sum_a N_a^u \boldsymbol{\delta u_a^e} \\ \boldsymbol{u^e} &= \sum_a N_a^u \boldsymbol{u_a^e} \\ \boldsymbol{\delta p^e} &= \sum_a N_a^p \boldsymbol{\delta p_a^e} \\ \boldsymbol{p^e} &= \sum_a N_a^p \boldsymbol{p_a^e} \\ \delta\Pi^e &= \sum_a N_a^{\Pi} \delta\Pi_a^e \\ \Pi^e &= \sum_a N_a^{\Pi} \Pi_a^e \end{aligned} \tag{A.3}$$

with a referring to nodal values and $\boldsymbol{N^u}$, $\boldsymbol{N^p}$ and $\boldsymbol{N^{\Pi}}$ being the mechanical, polarisation and pressure shape functions, respectively.

The time derivation of a generic variable $\bullet$ is computed as $\frac{\partial \bullet}{\partial t} = \frac{\bullet - \bullet^t}{\Delta t}$, with $\bullet$ and $\bullet^t$ being the current variable and the variable from the previous time step. Next, the weak forms of the residuals are obtained integrating within the reference (undeformed) configuration Ω_o as:

$$\begin{aligned} Res_{ia}^u &= \int_{\Omega_o} h_o P_{ij} N_{a,J}^u J dV + \int_{\Omega_o} \zeta \frac{u_i - u_i^t}{\Delta t} N_a^u J dV \\ &\quad - \int_{\Omega_o} \tilde{f} p_i N_a^u J dV = 0 \\ Res_{ia}^p &= \int_{\Omega_o} \frac{p_i - p_i^t}{\Delta t} N_a^p J dV + \int_{\Omega_o} \kappa p_{i,J} F_{Kj}^{-1} N_{a,J}^p F_{Kj}^{-1} J dV \\ &\quad + \int_{\Omega_o} \gamma E_s N_{a,I}^p F_{Ii}^{-1} J dV = 0 \\ Res_a^{\Pi} &= \int_{\Omega_o} \Pi N_a^{\Pi}\,(J-1)\, dV = 0 \end{aligned} \tag{A.4}$$

where $\boldsymbol{P} = J\boldsymbol{\sigma}\boldsymbol{F^{-T}}$ is the first Piola–Kirchhoff stress tensor. Note that the residual Res^{Π} imposes $J = 1$ all along the problem integration.

A.3. Implicit integration algorithm

We integrate the problem along time making use of an incremental iterative Newton–Raphson method that reduces the total residual to zero:

$$\begin{pmatrix} \boldsymbol{Res^u} \\ \boldsymbol{Res^p} \\ \boldsymbol{Res^{\Pi}} \end{pmatrix} + \begin{pmatrix} \boldsymbol{K^{uu}} & \boldsymbol{K^{up}} & \boldsymbol{K^{u\Pi}} \\ \boldsymbol{K^{pu}} & \boldsymbol{K^{pp}} & \boldsymbol{K^{p\Pi}} \\ \boldsymbol{K^{\Pi u}} & \boldsymbol{K^{\Pi p}} & \boldsymbol{K^{\Pi\Pi}} \end{pmatrix} \begin{pmatrix} \boldsymbol{du} \\ \boldsymbol{dp} \\ \boldsymbol{d\Pi} \end{pmatrix} = \boldsymbol{0} \tag{A.5}$$

where $\boldsymbol{K^{ij}}$ are the stiffness matrices. These matrices can be derived from the residuals as:

$$K^{uu}_{iakb} = \frac{\partial Res^u_{ia}}{\partial u_{kb}} = \int_\Omega \left(\frac{\partial P_{ij}}{\partial F_{kL}} h_o J N^u_{a,J} N^u_{b,L} + h_o P_{ij} N^u_{a,J} \frac{\partial J}{\partial F_{kL}} N^u_{b,L} \right) dV + \int_\Omega \left(\frac{\zeta \delta_{ik}}{\Delta t} J N^u_a N^u_b + \zeta \frac{u_i - u^t_i}{\Delta t} N^u_a \frac{\partial J}{\partial F_{kL}} N^u_{b,L} \right) dV - \int_\Omega \left(\frac{\partial \tilde{f}}{\partial F_{kL}} p_i J N^u_a N^u_{b,L} + \tilde{f} p_i N^u_a \frac{\partial J}{\partial F_{kL}} N^u_{b,L} \right) dV$$

$$K^{up}_{iakb} = \frac{\partial Res^u_{ia}}{\partial p_{kb}} = \int_\Omega \tilde{f} \delta_{ik} J N^u_a N^p_b dV$$

$$K^{u\Pi}_{iab} = \frac{\partial Res^u_{ia}}{\partial \Pi_b} = 0$$

$$K^{pp}_{iakb} = \frac{\partial Res^p_{ia}}{\partial p_{kb}} = \int_\Omega \frac{\delta_{ik}}{\Delta t} N^p_a N^p_b dV + \int_\Omega \kappa \delta_{ik} N^p_{a,J} F^{-1}_{Kj} N^p_{b,J} F^{-1}_{Kj} dV$$

$$K^{pu}_{iakb} = \frac{\partial Res^p_{ia}}{\partial u_{kb}} = \int_\Omega \frac{p_i - p^t_i}{\Delta t} N^p_a \frac{\partial J}{\partial F_{kL}} N^u_{b,L} dV + \int_{\Omega_o} \left(\frac{\partial \left(F^{-1}_{Kj} F^{-1}_{Kj} \right)}{\partial u_{kb}} \kappa p_{i,J} J N^p_{a,J} + \kappa p_{i,J} F^{-1}_{Kj} N^p_{a,J} F^{-1}_{Kj} \frac{\partial J}{\partial F_{kL}} N^u_{b,L} \right) dV + \int_{\Omega_o} \left(\frac{\partial \left(F^{-1}_{li} E_s \right)}{\partial u_{kb}} \gamma J N^p_{a,I} + \gamma E_s N^p_{a,I} F^{-1}_{li} \frac{\partial J}{\partial F_{kL}} N^u_{b,L} \right) dV$$

$$K^{p\Pi}_{iab} = \frac{\partial Res^p_{ia}}{\partial \Pi_b} = 0$$

$$K^{\Pi\Pi}_{ab} = \frac{\partial Res^\Pi_a}{\partial \Pi_b} = \int_\Omega N^\Pi_b N^\Pi_a \left(J - 1 \right) dV$$

$$K^{\Pi u}_{akb} = \frac{\partial Res^\Pi_a}{\partial u_{kb}} = \int_{\Omega_o} \frac{\partial J}{\partial F_{kL}} N^u_{b,L} \Pi N^\Pi_a dV$$

$$K^{\Pi p}_{aib} = \frac{\partial Res^\Pi_a}{\partial p_{ib}} = 0 \tag{A.6}$$

Note that the terms $\frac{\partial P_{ij}}{\partial F_{kL}}$, $\frac{\partial \tilde{f}}{\partial F_{kL}}$ and $\frac{\partial \left(F^{-1}_{li} E_s \right)}{\partial u_{kb}}$ depends on the constitutive equations chosen, while the remaining terms $\frac{\partial \left(F^{-1}_{Kj} F^{-1}_{Kj} \right)}{\partial u_{kb}}$ and $\frac{\partial J}{\partial F_{kL}}$ are general and can be found in the literature (see, for example, Ref. [35]).

References

[1] B. Ladoux, R.-M. Mège, Mechanobiology of collective cell behaviours, Nat. Rev. Mol. Cell Biol. 18 (12) (2017) 743–757, http://dx.doi.org/10.1038/nrm.2017.98.

[2] S. Begnaud, T. Chen, D. Delacour, R.-M. Mège, B.t. Ladoux, Mechanics of epithelial tissues during gap closure, Curr. Opin. Cell Biol. 42 (2016) 52—62, http://dx.doi.org/10.1016/j.ceb.2016.04.006, URL https://europepmc.org/articles/PMC5428743.

[3] R. Alert, X. Trepat, Physical models of collective cell migration, Ann. Rev. Condens. Matter Phys. 11 (1) (2020) 77–101, http://dx.doi.org/10.1146/annurev-conmatphys-031218-013516.

[4] W. Xi, T.B. Saw, D. Delacour, C.T. Lim, B. Ladoux, Material approaches to active tissue mechanics, Nat. Rev. Mater. 4 (1) (2019) 23–44, http://dx.doi.org/10.1038/s41578-018-0066-z.

[5] S. Garcia, E. Hannezo, J. Elgeti, J.-F. Joanny, P. Silberzan, N.S. Gov, Physics of active jamming during collective cellular motion in a monolayer, Proc. Natl. Acad. Sci. 112 (50) (2015) 15314–15319, http://dx.doi.org/10.1073/pnas.1510973112, URL https://www.pnas.org/content/112/50/15314.

[6] V. Maruthamuthu, B. Sabass, U.S. Schwarz, M.L. Gardel, Cell-ECM traction force modulates endogenous tension at cell–cell contacts, Proc. Natl. Acad. Sci. 108 (12) (2011) 4708–4713, http://dx.doi.org/10.1073/pnas.1011123108, URL https://www.pnas.org/content/108/12/4708.

[7] A. Elosegui-Artola, X. Trepat, P. Roca-Cusachs, Control of mechanotransduction by molecular clutch dynamics, Trends Cell Biol. 28 (5) (2018) 356–367, http://dx.doi.org/10.1016/j.tcb.2018.01.008.

[8] P. Bun, J. Liu, H. Turlier, Z. Liu, K. Uriot, J.-F. Joanny, M. Coppey-Moisan, Mechanical checkpoint for persistent cell polarization in adhesion-naive fibroblasts, Biophys. J. 107 (2) (2014) 324–335, http://dx.doi.org/10.1016/j.bpj.2014.05.041.

[9] M.T. Breckenridge, R.A. Desai, M.T. Yang, J. Fu, C.S. Chen, Substrates with engineered step changes in rigidity induce traction force polarity and durotaxis, Cell. Mol. Bioeng. 7 (1) (2014) 26–34, http://dx.doi.org/10.1007/s12195-013-0307-6.

[10] M. Gupta, B.L. Doss, L. Kocgozlu, M. Pan, R.-M. Mège, A. Callan-Jones, R. Voituriez, B. Ladoux, Cell shape and substrate stiffness drive actin-based cell polarity, Phys. Rev. E 99 (2019) 012412, http://dx.doi.org/10.1103/PhysRevE.99.012412, URL https://link.aps.org/doi/10.1103/PhysRevE.99.012412.

[11] N.A. Kurniawan, C.V. Bouten, Mechanobiology of the cell–matrix interplay: Catching a glimpse of complexity via minimalistic models, Extreme Mech. Lett. 20 (2018) 59–64, http://dx.doi.org/10.1016/j.eml.2018.01.004, URL http://www.sciencedirect.com/science/article/pii/S2352431617301864.

[12] X. Ma, M.E. Schickel, M.D. Stevenson, A.L. Sarang-Sieminski, K.J. Gooch, S.N. Ghadiali, R.T. Hart, Fibers in the extracellular matrix enable long-range stress transmission between cells, Biophys. J. 104 (7) (2013) 1410–1418, http://dx.doi.org/10.1016/j.bpj.2013.02.017, URL http://www.sciencedirect.com/science/article/pii/S0006349513002075.

[13] H. Wang, A. Abhilash, C.S. Chen, R.G. Wells, V.B. Shenoy, Long-range force transmission in fibrous matrices enabled by tension-driven alignment of fibers, Biophys. J. 107 (11) (2014) 2592–2603, http://dx.doi.org/10.1016/j.bpj.2014.09.044, URL http://www.sciencedirect.com/science/article/pii/S0006349514011096.

[14] A. Malandrino, M. Mak, R.D. Kamm, E. Moeendarbary, Complex mechanics of the heterogeneous extracellular matrix in cancer, Extreme Mech. Lett. 21 (2018) 25–34, http://dx.doi.org/10.1016/j.eml.2018.02.003, URL http://www.sciencedirect.com/science/article/pii/S2352431617301694.

[15] C.-M. Lo, H.-B. Wang, M. Dembo, Y. li Wang, Cell movement is guided by the rigidity of the substrate, Biophys. J. 79 (1) (2000) 144–152, http://dx.doi.org/10.1016/S0006-3495(00)76279-5, URL http://www.sciencedirect.com/science/article/pii/S0006349500762795.

[16] R. Sunyer, V. Conte, J. Escribano, A. Elosegui-Artola, A. Labernadie, L. Valon, D. Navajas, J.M. García-Aznar, J.J. Muñoz, P. Roca-Cusachs, X. Trepat, Collective cell durotaxis emerges from long-range intercellular force transmission, Science 353 (6304) (2016) 1157–1161, http://dx.doi.org/10.1126/science.aaf7119, URL https://science.sciencemag.org/content/353/6304/1157.

[17] F.O. Ribeiro, M.J. Gómez-Benito, J. Folgado, P.R. Fernandes, J.M. García-Aznar, Computational model of mesenchymal migration in 3D under chemotaxis, Comput. Methods Biomech. Biomed. Eng. 20 (1) (2017) 59–74, http://dx.doi.org/10.1080/10255842.2016.1198784.

[18] Y. Cao, E. Ghabache, Y. Miao, C. Niman, H. Hakozaki, S.L. Reck-Peterson, P.N. Devreotes, W.-J. Rappel, A minimal computational model for three-dimensional cell migration, J. R. Soc. Interface 16 (161) (2019) 20190619, http://dx.doi.org/10.1098/rsif.2019.0619, URL https://royalsocietypublishing.org/doi/abs/10.1098/rsif.2019.0619.

[19] S. Banerjee, K.J.C. Utuje, M.C. Marchetti, Propagating stress waves during epithelial expansion, Phys. Rev. Lett. 114 (2015) 228101, http://dx.doi.org/10.1103/PhysRevLett.114.228101, URL https://link.aps.org/doi/10.1103/PhysRevLett.114.228101.

[20] R. Alert, C. Blanch-Mercader, J. Casademunt, Active fingering instability in tissue spreading, Phys. Rev. Lett. 122 (2019) 088104, http://dx.doi.org/10.1103/PhysRevLett.122.088104, URL https://link.aps.org/doi/10.1103/PhysRevLett.122.088104.

[21] S. Banerjee, M.C. Marchetti, Continuum models of collective cell migration, in: C.A.M. La Porta, S. Zapperi (Eds.), Cell Migrations: Causes and Functions, Springer International Publishing, Cham, 2019, pp. 45–66, http://dx.doi.org/10.1007/978-3-030-17593-1_4.

[22] I. González-Valverde, J.M.G. a Aznar, Mechanical modeling of collective cell migration: An agent-based and continuum material approach, Comput. Methods Appl. Mech. Engrg. 337 (2018) 246–262, http://dx.doi.org/10.1016/j.cma.2018.03.036, URL http://www.sciencedirect.com/science/article/pii/S0045782518301609.

[23] J. Escribano, R. Sunyer, M.T. Sánchez, X. Trepat, P. Roca-Cusachs, J.M. García-Aznar, A hybrid computational model for collective cell durotaxis, Biomech. Model. Mechanobiol. 17 (4) (2018) 1037–1052, http://dx.doi.org/10.1007/s10237-018-1010-2.

[24] D. Garcia-Gonzalez, C.M. Landis, Magneto-diffusion-viscohyperelasticity for magneto-active hydrogels: Rate dependences across time scales, J. Mech. Phys. Solids 139 (2020) 103934, http://dx.doi.org/10.1016/j.jmps.2020.103934, URL http://www.sciencedirect.com/science/article/pii/S0022509620301708.

[25] L. Trichet, J. Le Digabel, R.J. Hawkins, S.R.K. Vedula, M. Gupta, C. Ribrault, P. Hersen, R. Voituriez, B. Ladoux, Evidence of a large-scale mechanosensing mechanism for cellular adaptation to substrate stiffness, Proc. Natl. Acad. Sci. 109 (18) (2012) 6933–6938, http://dx.doi.org/10.1073/pnas.1117810109, URL https://www.pnas.org/content/109/18/6933.

[26] J. Li, D. Han, Y.-P. Zhao, Kinetic behaviour of the cells touching substrate: the interfacial stiffness guides cell spreading, Sci. Rep. 4 (1) (2014) 3910, http://dx.doi.org/10.1038/srep03910.

[27] M. Gupta, B.R. Sarangi, J. Deschamps, Y. Nematbakhsh, A. Callan-Jones, F. Margadant, R.-M. Mège, C.T. Lim, R. Voituriez, B. Ladoux, Adaptive rheology and ordering of cell cytoskeleton govern matrix rigidity sensing, Nature Commun. 6 (1) (2015) 7525, http://dx.doi.org/10.1038/ncomms8525.

[28] R. Alert, J. Casademunt, Role of substrate stiffness in tissue spreading: Wetting transition and tissue durotaxis, Langmuir 35 (23) (2019) 7571–7577, http://dx.doi.org/10.1021/acs.langmuir.8b02037.

[29] C. Pérez-González, R. Alert, C. Blanch-Mercader, M. Gómez-González, T. Kolodziej, E. Bazellieres, J. Casademunt, X. Trepat, Active wetting of epithelial tissues, Nat. Phys. 15 (1) (2019) 79–88, http://dx.doi.org/10.1038/s41567-018-0279-5.

[30] S. Park, J. Tao, L. Sun, C.-M. Fan, Y. Chen, An economic, modular, and portable skin viscoelasticity measurement device for in situ longitudinal studies, Molecules 24 (5) (2019) 907, http://dx.doi.org/10.3390/molecules24050907.

[31] C. Blanch-Mercader, R. Vincent, E. Bazellières, X. Serra-Picamal, X. Trepat, J. Casademunt, Effective viscosity and dynamics of spreading epithelia: a solvable model, Soft Matter 13 (2017) 1235–1243, http://dx.doi.org/10.1039/C6SM02188C.

[32] O. Cochet-Escartin, J. Ranft, P. Silberzan, P. Marcq, Border forces and friction control epithelial closure dynamics, Biophys. J. 106 (1) (2014) 65–73, http://dx.doi.org/10.1016/j.bpj.2013.11.015.

[33] D. Joaquin, M. Grigola, G. Kwon, C. Blasius, Y. Han, D. Perlitz, J. Jiang, Y. Ziegler, A. Nardulli, K.J. Hsia, Cell migration and organization in three-dimensional in vitro culture driven by stiffness gradient, Biotechnol. Bioeng. 113 (11) (2016) 2496–2506, http://dx.doi.org/10.1002/bit.26010, URL https://onlinelibrary.wiley.com/doi/abs/10.1002/bit.26010.

[34] A. Nestor-Bergmann, G.A. Stooke-Vaughan, G.K. Goddard, T. Starborg, O.E. Jensen, S. Woolner, Decoupling the roles of cell shape and mechanical stress in orienting and cueing epithelial mitosis, Cell Rep. 26 (8) (2019) 2088 – 2100.e4, http://dx.doi.org/10.1016/j.celrep.2019.01.102, URL http://www.sciencedirect.com/science/article/pii/S2211124719301391.

[35] M.T. Kwong, F. Bianchi, M. Malboubi, J.A.G. a Grajales, L. Homsi, M. Thompson, H. Ye, L. Noels, A. Jérusalem, 3D finite element formulation for mechanical–electrophysiological coupling in axonopathy, Comput. Methods Appl. Mech. Engrg. 346 (2019) 1025–1050, http://dx.doi.org/10.1016/j.cma.2018.09.006, URL http://www.sciencedirect.com/science/article/pii/S0045782518304493.